DISCRETIZATION OF A HARMONIC MEASURE PROBLEM AND SPANDREL

AUSTIN ANDERSON

Abstract. It appears difficult to make precise estimates of the harmonic measure of certain starlike domains in the complex plane. Based on work of Chelkak and Smirnov, discretization of the problem using Brownian motion on isoradial graphs may be a useful tool. A spandrel problem about infinite graphs arises.

1. Introduction

Let Ω be a slitted starlike domain in $\mathbb{C}$ with channels of monotone width, symmetric with respect to the real axis. Denoting $\mathbb{D} = \{z \in \mathbb{C} : |z| < 1\}$, an example is given by $f(\mathbb{D})$ for a Riemann map f illustrated below.

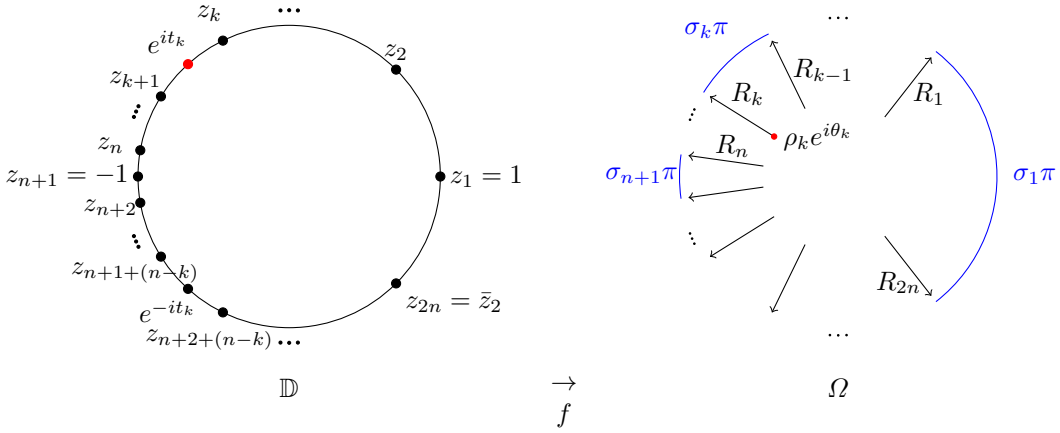

The explicit formula

$$f(z) = z \prod_{j=1}^{2n} (1 - \bar{z}_j z)^{-\sigma_j} \tag{1.1}$$

for f can be given; see [2, Thm 3.18].

The points z_k correspond to angles σ_k dependent on ρ_k, the slits' starting moduli. The symmetrical setup gives the following equations for $k = 2, 3, ..., n$.

$$z_{2n+2-k} = \bar{z}_k.$$

$$\sigma_{2n+2-k} = \sigma_k.$$

$$\exp(it_{2n+1-k}) = \exp(-it_k).$$

Date: September 6, 2024.
2000 *Mathematics Subject Classification.* Primary:
Key words and phrases. Harmonic measure, isoradial graph, starlike, Brownian motion .

$$\rho_{2n+1-k} = \rho_k.$$

If we require that $\rho_k = \rho_j$ for all j, k, we can prescribe either $\{z_k\}$ or $\{\sigma_k\}$, but their precise relationship is not obvious. Denote the arc lengths on the unit circle from z_k to z_{k+1} by

$$\{\omega_k = |(z_k, z_{k+1})|\},$$

and it follows that ω_k is the harmonic measure of the slit R_k in Ω. One natural question is the following.

Question 1.1. *Does $\{\omega_k\}_1^n$ being monotone imply $\{\sigma_k\}_1^n$ are monotone, and vice versa?*

We conjecture that the answer is yes, but a proof using classic geometric function theory eludes us.

2. Discretization

For convenience let us reflect Ω about the imaginary axis and make the slits start on the unit circle. For symmetric slits

$$S_k = \{re^{\pm i\theta_k} : r \geq 1\} \tag{2.1}$$

satisfying $\theta_0 = 0 < \theta_1 < \theta_2 < ... < \theta_N$ with $(\theta_k - \theta_{k-1}) \leq (\theta_{k+1} - \theta_k)$ for all $k = 1, ..., N-1$, define

$$\Omega = \mathbb{C} \setminus \left(\cup_{k=0}^N S_k\right). \tag{2.2}$$

We also denote the channels

$$C_k = \{re^{\pm i\theta} : r > 1, \theta_k < \theta < \theta_{k+1}\}. \tag{2.3}$$

Following [1], for each $\delta > 0$, we define an isoradial graph Γ^δ to approximate compact subsets of Ω. An *isoradial* graph is planar and consists of faces that are all inscribed in circles of the same radius. In [1], an infinite graph is used, which has the advantage of ensuring a connected boundary exists for any bounded subset. Here, we use finite Γ^δ and eventually describe the boundary explicitly; see Question (2.3) below.

We may assume $\delta^2 = 2\pi/m$ for some integer m. The vertices along rays spaced by $\Delta\theta = \delta^2$ can extend to radius $1/\delta$, creating graphs that fill Ω as δ tends to 0.

Specifying the moduli of the vertices, we begin with $r_0 = 0$. The isoradial property determines the following recursive formula for $r_j = r_j(\delta)$.

$$r_{j+1} = r_j \cos(\pi/m) + \sqrt{(r_j \cos(\pi/m))^2 - r_j^2 + \delta^2}, \tag{2.4}$$

which gives the moduli of the circle centers of the graph faces for odd indices, and the moduli of the vertices for even indices. (We stop the recursion once the term in the square root is negative. It is not obvious that $\#\{r_n\}$ is finite, but it turns out to be so for the simulated values of δ in question, and in any case we can eschew vertices near the edge without affecting our results.)

Thus we denote the even indices $\{r_{2n}\}$, and have the vertices

$$V(\Gamma^\delta) = \{r_j e^{i\ell\delta^2} : \ell = 1, ..., m \qquad r_j \in \{r_{2n}\}\}. \tag{2.5}$$

The edges $E(\Gamma^\delta)$ are between vertex neighbors who share either modulus or argument.

Note again that $r_j\Delta\theta < \delta$, i.e., $r_j < 1/\delta$, is a condition on the maximum r_j, which we denote $r_{\max}^\delta$.

FIGURE 1. Graph shown in black. Circle centers are pink.

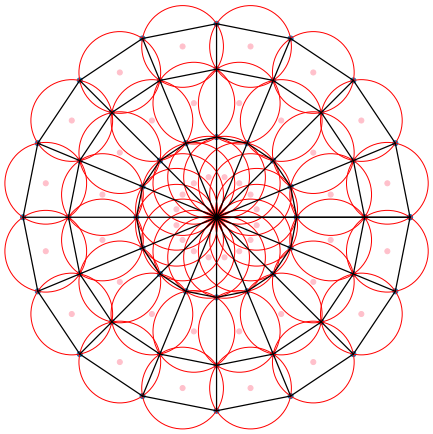

FIGURE 2. Isoradial polar graph with $m = 16$.

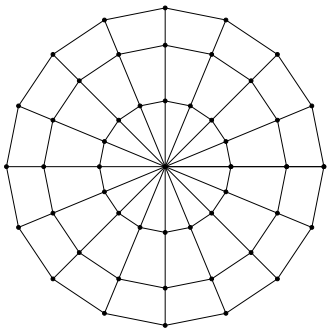

FIGURE 3. Isoradial polar graph with $m = 64$.

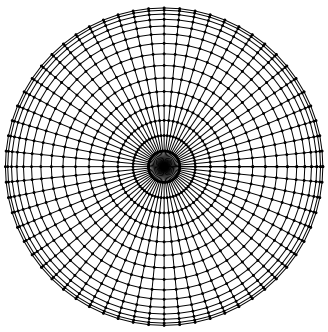

As $\delta \to 0$, Ω will be approximated by successively larger and finer grids Ω^δ with vertices

$$V_{\Omega^\delta} = V(I^\delta) \setminus S_{\Omega^\delta} \tag{2.6}$$

where the boundary S_{Ω^δ} is the closest approximation to the slits S, as we describe next.

For every slit tip $e^{i\theta_k}$ there exists a nearest set of vertices $\{\gamma_k^\delta\} \subset \{V(\Gamma^\delta)\}$ such that

$$\gamma_k^\delta \to e^{i\theta_k} \text{ as } \delta \to 0, \tag{2.7}$$

with a symmetric argument for each $e^{-i\theta_k}$. The discrete slit

$$(S_k)_{\Omega^\delta} = \{v \in V(\Gamma^\delta) : \arg v = \arg \gamma_k^\delta, |v| \geq |\gamma_k^\delta|\}, \tag{2.8}$$

and the boundary $\partial\Omega_\delta = \partial\Omega_{\Gamma^\delta} = \partial\Omega_\Gamma^\delta$ is a connected set of vertices intersecting

$$S_{\Omega^\delta} = \cup_{k=0}^N (S_k)_{\Omega^\delta}. \tag{2.9}$$

Also, the moduli of γ_k^δ are the same for all k, and approach 1 as $\delta \to 0$. Thus, for each δ we have the disjoint union

$$\{v \in V(\Gamma^\delta) : |v| = |\gamma_k^\delta|\} = \{\gamma_k^\delta\} \sqcup \{v^\delta\}, \tag{2.10}$$

with the vertices denoting channel openings

$$\{v^\delta\} = \cup_k \{v_{k,\ell}^\delta, \quad \ell = 1, ..., n_k^\delta\}. \tag{2.11}$$

The double index on $v_{k,\ell}^\delta$ will be used below in Brownian motion estimates. n_k^δ measures the discrete channel width, and

$$n_k^\delta \approx (\theta_k - \theta_{k-1})/\delta^2, \tag{2.12}$$

with $n_k^\delta \leq n_{k+1}^\delta$ for all k. For small enough δ, each channel C_k corresponds to interior vertices extending to $r_{\max}^\delta$. (If δ is not smaller than the kth channel width, then $n_k^\delta = 0$, and the channel will be excluded from the discrete approximation.) So the discrete channels are

$$(C_k)_{\Omega^\delta} = \cup_{\ell=1}^{n_k} \{v \in V(\Gamma^\delta) : \arg v = \arg v_{k,\ell}^\delta, \quad |v_{k,\ell}^\delta| \leq |v| < r_{\max}^\delta\}. \tag{2.13}$$

Our discrete domain Ω_Γ^δ consists of the channels together with the approximation of the unit disk

$$\mathbb{D}^\delta = \{v \in V(\Gamma^\delta) : |v| \leq |v_{k,\ell}^\delta| \approx 1\}, \tag{2.14}$$

along with a boundary depending on the slits.

I.e.,

$$\text{int}\Omega_\Gamma^\delta = \left(\mathbb{D}^\delta \setminus \{\gamma_k^\delta\}\right) \bigcup \cup_k (C_k)_{\Omega^\delta}, \tag{2.15}$$

and

$$\partial\Omega_\Gamma^\delta = \{\gamma_k\} \cup \{(S_k)_{\Omega^\delta} : n_k \neq 0\} \cup \{v : \arg v = \arg v_{k,\ell}^\delta, |v| = r_{\max}^\delta\}. \tag{2.16}$$

FIGURE 4. Example. Boundary shown in black.

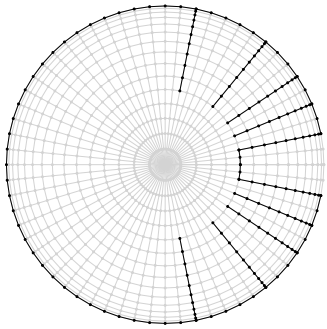

FIGURE 5. Example. Vertex labelling.

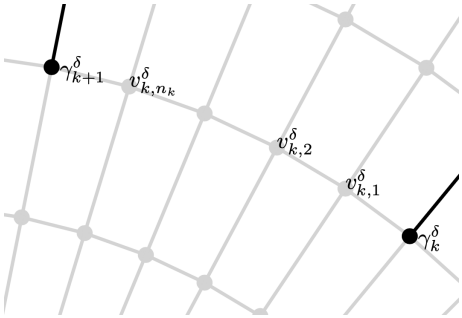

Random walk

In essence, we employ a discrete version of the famous Kakutani theorem linking Brownian motion with harmonic measure. The fairly clear intuition is that a random walk has higher probability of landing in a big channel than a small one, thereby achieving the monotonicity conjecture answering Question 1.1. We seek to prove that a Brownian traveller on our discrete polar graph with monotone channels maintains a monotonicity of probable location at every step.

As in [1, p. 1593], we define a random walk RW on Ω^δ_Γ, where

$$RW(t+1) = RW(t) + \xi_{RW(t)} \tag{2.17}$$

and for the neighbors u_j of a vertex v with angles θ_j

$$\mathbf{P}(\xi_v = u_k - v) = \frac{\tan\theta_k}{\sum_j \tan\theta_j}. \tag{2.18}$$

We will start at the origin, assuming $RW(0) = 0$. For example, in the first circle

$$|u| = r_2^\delta \Rightarrow \mathbf{P}(RW(1) = u) = 1/m. \tag{2.19}$$

Apart from 0, all interior vertices have 4 neighbors. Also, θ_u is invariant under rotations. For $B \subset \operatorname{int}\Omega^\delta_\Gamma$, we define the discrete harmonic measure $\omega^\delta(0; B; \Omega^\delta_\Gamma)$ to be the probability that the random walk hits B before any other part of the boundary.

Define the channel boundaries as

$$\partial(C_k)_{\Omega^\delta} = \{v \in \partial\Omega^\delta_\Gamma : (v,u) \in E(\Gamma^\delta), \quad u \in (C_k)_{\Omega^\delta}\}. \tag{2.20}$$

Our main purpose here is to show that

$$\omega^\delta(0; \partial(C_k)_{\Omega^\delta}; \Omega^\delta_\Gamma) \le \omega^\delta(0; \partial(C_{k+1})_{\Omega^\delta}; \Omega^\delta_\Gamma), \tag{2.21}$$

implying the harmonic measures of channels are monotone like their widths.

The probability that RW will land on any vertex v comes from a Markov process encapsulated by a linear map M on the vertices in Ω^δ_Γ. Enumerate all the vertices,

and write M as a matrix where M_{ij} is the probability of moving from the ith vertex to the jth. Let $\mathbf{e_v}$ be the vector with all 0s except a 1 in the index corresponding to v. Then

$$\mathbf{P}(RW(t) = v) = \mathbf{e_v} \cdot M^t \mathbf{e_0}, \tag{2.22}$$

where M^t is a product of t copies of M, and the dot product extracts the value corresponding to v. Define M^0 to be the identity matrix, a square matrix with side length equal to the cardinality of Ω_Γ^δ.

The row corresponding to $v = 0$ in the enumeration will be a vector with m nonzero entries with value $1/m$, and the typical interior vertex will correspond to a row with exactly 4 nonzero entries with values around $1/4$ that add to 1. The row corresponding to a boundary vertex will have only one nonzero entry, which will be a 1 in the same column as row number. Evidently,

$$\lim_{t\to\infty} \mathbf{e_v} \cdot M^t \mathbf{e_0} \begin{cases} > 0, & v \in \partial\Omega_\Gamma^\delta \\ = 0, & v \in \mathrm{int}\Omega_\Gamma^\delta \end{cases}. \tag{2.23}$$

The crux of our argument is the following lemma. We need $v_{k,\ell}^\delta$ to range over all radii in Ω_Γ^δ. That is, (k,ℓ) dictates interior vertex argument, but refers to vertex of arbitrary radius. Thats not how it was defined above, but assuming it below seems ok for now.

Lemma 2.1. *For all $t, k \in \mathbb{N}$,*

$$\mathbf{P}(RW(t) = v_{k,\ell}^\delta) \le \min(\mathbf{P}(RW(t) = v_{k+1,\ell}^\delta), \mathbf{P}(RW(t) = v_{k+1,n_{k+1}-\ell+1}^\delta)). \tag{2.24}$$

Proof. We proceed by induction on t. The base case $t = 0$ is clear since all the relevant quantities are 0. We will write

$$Mvu = \mathbf{P}(RW(t+1) = v \,|\, RW(t) = u) \tag{2.25}$$

as a way to refer to entries of the Markov matrix. For every vertex except the origin, we have the four term Markov process equation

$$\mathbf{P}(RW(t+1) = v) = Mvv_l \mathbf{P}(RW(t) = v_l) + Mvv_r \mathbf{P}(RW(t) = v_r) \tag{2.26}$$

$$+ Mvv_u \mathbf{P}(RW(t) = v_u) + Mvv_d \mathbf{P}(RW(t) = v_d). \tag{2.27}$$

Here we have denoted the neighbor vertices v_l, v_r, v_u, v_d with a picture of left, right, up, and down in mind. Rotational invariance and monotonicity of n_k gives

$$Mv_{k,\ell}^\delta (v_{k,\ell}^\delta)_a = Mv_{k+1,\ell}^\delta (v_{k+1,\ell}^\delta)_a, \quad a = l, r, u, d, \tag{2.28}$$

except when $n_{k+1} > n_k = \ell$ and $a = l$, which is when there is a boundary to the left in the kth channel but not the $k+1$st. In this case, $Mv_{k,n_k}^\delta (v_{k,n_k}^\delta)_l = 0$, so the proof below holds. We also require comparison via intrachannel reflection, which gives

$$Mv_{k,\ell}^\delta (v_{k,\ell}^\delta)_r = Mv_{k+1,n_{k+1}-\ell+1}^\delta (v_{k+1,n_{k+1}-\ell+1}^\delta)_l, \tag{2.29}$$

$$Mv_{k,\ell}^\delta (v_{k,\ell}^\delta)_l = Mv_{k+1,n_{k+1}-\ell+1}^\delta (v_{k+1,n_{k+1}-\ell+1}^\delta)_r. \tag{2.30}$$

Then using the inductive assumption and 2.28,

$$\mathbf{P}(RW(t+1)=v^\delta_{k,\ell}) = Mv^\delta_{k,\ell}(v^\delta_{k,\ell})_l\mathbf{P}(RW(t)=(v^\delta_{k,\ell})_l) \tag{2.31}$$

$$+ Mv^\delta_{k,\ell}(v^\delta_{k,\ell})_r\mathbf{P}(RW(t)=(v^\delta_{k,\ell})_r) \tag{2.32}$$

$$+ Mv^\delta_{k,\ell}(v^\delta_{k,\ell})_u\mathbf{P}(RW(t)=(v^\delta_{k,\ell})_u) \tag{2.33}$$

$$+ Mv^\delta_{k,\ell}(v^\delta_{k,\ell})_d\mathbf{P}(RW(t)=(v^\delta_{k,\ell})_d) \tag{2.34}$$

$$\le Mv^\delta_{k+1,\ell}(v^\delta_{k+1,\ell})_l\mathbf{P}(RW(t)=(v^\delta_{k+1,\ell})_l) \tag{2.35}$$

$$+ Mv^\delta_{k+1,\ell}(v^\delta_{k+1,\ell})_r\mathbf{P}(RW(t)=(v^\delta_{k+1,\ell})_r) \tag{2.36}$$

$$+ Mv^\delta_{k+1,\ell}(v^\delta_{k+1,\ell})_u\mathbf{P}(RW(t)=(v^\delta_{k+1,\ell})_u) \tag{2.37}$$

$$+ Mv^\delta_{k+1,\ell}(v^\delta_{k+1,\ell})_d\mathbf{P}(RW(t)=(v^\delta_{k+1,\ell})_d) \tag{2.38}$$

$$= \mathbf{P}(RW(t+1)=v^\delta_{k+1,\ell}). \tag{2.39}$$

The inductive assumption implies that

$$\mathbf{P}(RW(t)=(v^\delta_{k,\ell})_l) \le \mathbf{P}(RW(t)=(v^\delta_{k+1,n_k+1-\ell})_r), \tag{2.40}$$

except in the case that $(v^\delta_{k,\ell})_l$ is the boundary. However, in that case $Mv^\delta_{k,\ell}(v^\delta_{k,\ell})_l$ is 0. So we also have

$$\mathbf{P}(RW(t+1)=v^\delta_{k,\ell}) = Mv^\delta_{k,\ell}(v^\delta_{k,\ell})_l\mathbf{P}(RW(t)=(v^\delta_{k,\ell})_l) \tag{2.41}$$

$$+ Mv^\delta_{k,\ell}(v^\delta_{k,\ell})_r\mathbf{P}(RW(t)=(v^\delta_{k,\ell})_r) \tag{2.42}$$

$$+ Mv^\delta_{k,\ell}(v^\delta_{k,\ell})_u\mathbf{P}(RW(t)=(v^\delta_{k,\ell})_u) \tag{2.43}$$

$$+ Mv^\delta_{k,\ell}(v^\delta_{k,\ell})_d\mathbf{P}(RW(t)=(v^\delta_{k,\ell})_d) \tag{2.44}$$

$$\le Mv^\delta_{k+1,n_k+1-\ell}(v^\delta_{k+1,n_k+1-\ell})_r\mathbf{P}(RW(t)=(v^\delta_{k+1,n_k+1-\ell})_r) \tag{2.45}$$

$$+ Mv^\delta_{k+1,n_k+1-\ell}(v^\delta_{k+1,n_k+1-\ell})_l\mathbf{P}(RW(t)=(v^\delta_{k+1,n_k+1-\ell})_l) \tag{2.46}$$

$$+ Mv^\delta_{k+1,n_k+1-\ell}(v^\delta_{k+1,n_k+1-\ell})_u\mathbf{P}(RW(t)=(v^\delta_{k+1,n_k+1-\ell})_u) \tag{2.47}$$

$$+ Mv^\delta_{k+1,n_k+1-\ell}(v^\delta_{k+1,n_k+1-\ell})_d\mathbf{P}(RW(t)=(v^\delta_{k+1,n_k+1-\ell})_d) \tag{2.48}$$

$$= \mathbf{P}(RW(t+1)=v^\delta_{k+1,n_k+1-\ell}). \tag{2.49}$$

□

Having established a monotone property on the interior vertices, we use it to do the same on the boundary slits.

Lemma 2.2. *For all $t, k \in \mathbb{N}$,*

$$\mathbf{P}(RW(t)=\gamma^\delta_k) \le \mathbf{P}(RW(t)=\gamma^\delta_{k+1}). \tag{2.50}$$

Proof. Note, for example, that $(\gamma^\delta_k)_r = v^\delta_{k-1,n_{k-1}}$. The Markov equation is

$$\mathbf{P}(RW(t+1)=\gamma^\delta_k) = M\gamma^\delta_k v^\delta_{k-1,n_{k-1}}\mathbf{P}(RW(t)=v^\delta_{k-1,n_{k-1}}) \tag{2.51}$$

$$+ M\gamma^\delta_k v^\delta_{k,1}\mathbf{P}(RW(t)=v^\delta_{k,1}) \tag{2.52}$$

$$+ M\gamma^\delta_k(\gamma^\delta_k)_u\mathbf{P}(RW(t)=(\gamma^\delta_k)_u) \tag{2.53}$$

$$+ M\gamma^\delta_k(\gamma^\delta_k)_d\mathbf{P}(RW(t)=(\gamma^\delta_k)_d) \tag{2.54}$$

The last two terms are 0 down the slit, but we have to be careful about the tips and the rays inside the unit circle. It seems to me the inductive assumption takes care

of those cases. And the previous lemma takes care of the first two terms, although we must consider the case $k = 0$ where there may be no neighbor vertex to one side, or where, because of symmetry, we need not bother. Note also Figure 4 has an inaccuracy where it shows black vertices in corners which are unreachable, so the formal graph boundary excludes them. □

Spandrel

We use the term *spandrel* in the sense of evolutionary biology, rather than architecture. A question unimportant to the original goal of research, but curious in its own right, arose while we wrote code in Python and Sagemath to produce images of isoradial graphs. We were unable to find an algorithm that could generate an infinite graph fitting the starlike appropriate starlike property. Given $\delta > 0$, we define a *infinite dyadic polar isoradial starlike graph* to be an isoradial graph Γ^δ with the following properties:

(Dyadic) $v \in V(\Gamma^\delta)$ implies $\arg v = 2\pi/2^n$ for some integer n;
(Starlike) $re^{i\theta} \in V(\Gamma^\delta)$ implies $(r+\delta)e^{i\theta} \in V(\Gamma^\delta)$;
(Infinite) for all $r > 0$, there exists $v \in V(\Gamma^\delta)$ such that $|v| > r$.

Question 2.3. *Does an infinite dyadic polar isoradial starlike graph exist?*

We conjecture the answer is no, mostly because we failed to produce one. If $N(r)$ is the number of vertices on the polar graph with modulus r, a successful one would double N at every modulus in a cleverly chosen sequence $\{r_k\}$, which seems to be subject to too many constraints to exist. Below are some images created by our algorithms.

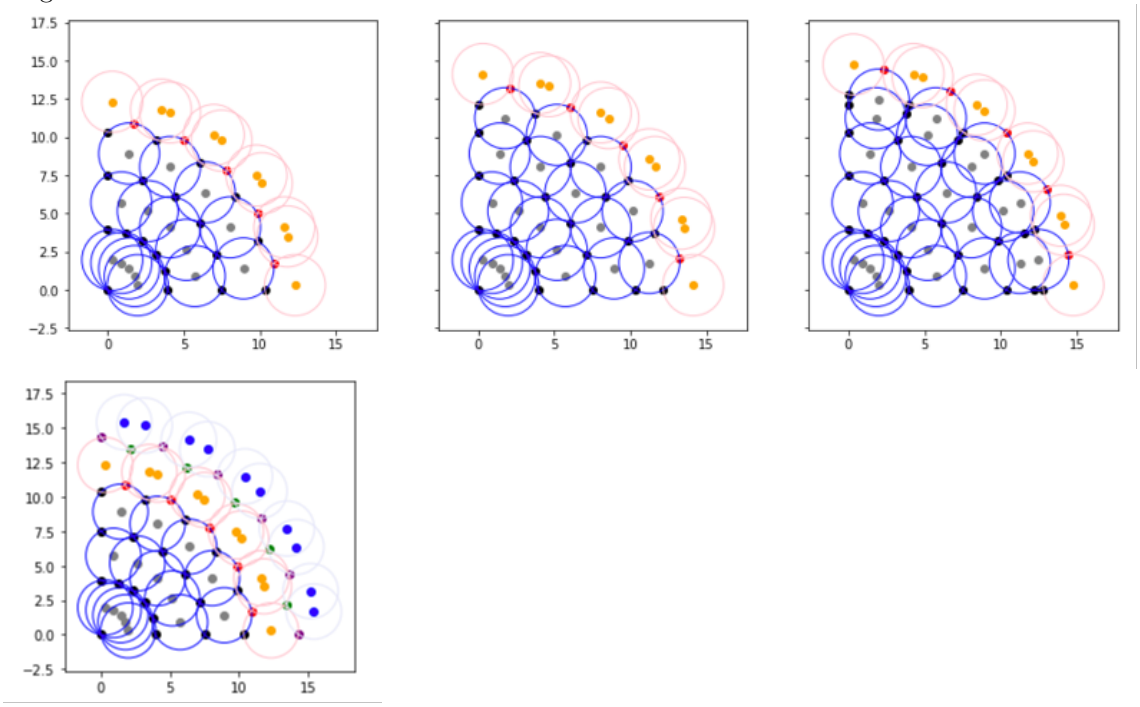

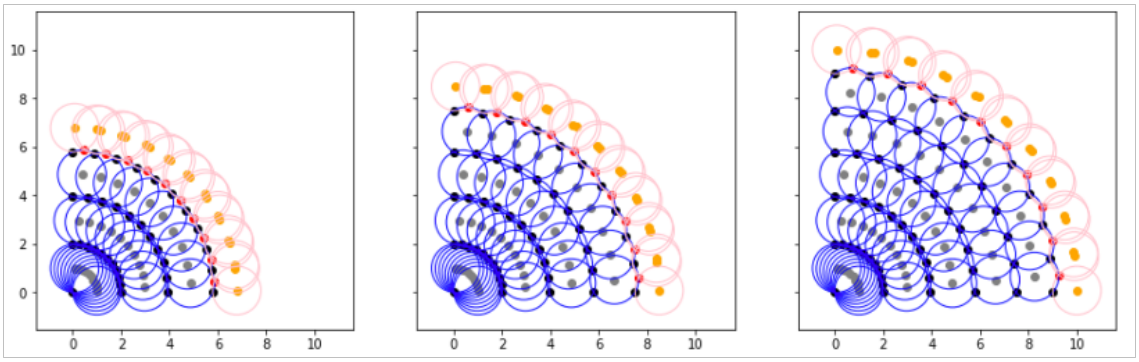
0
2
4
6
8
10

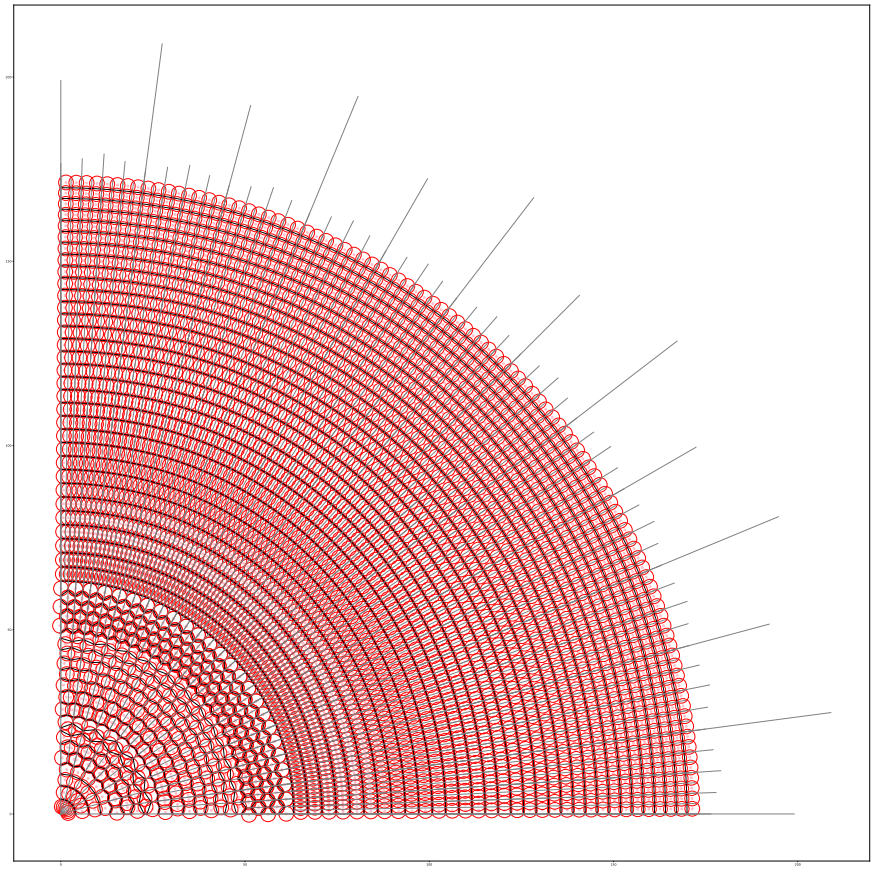

References

[1] D. Chelkak and S. Smirnov, *Discrete complex analysis on isoradial graphs*, Adv. Math 228 (2011), 1590–1630.
[2] Ch. Pommerenke, *Boundary Behavior of Conformal Maps*, Springer-Verlag 1992.

Department of Mathematics, University of Hawaii, Honolulu, Hawaii 96822
Email address: austina@hawaii.edu